V.M. GORKAVENKO,[1] YU.A. SITENKO,[2] O.B. STEPANOV[2]

[1] Faculty of Physics, Taras Shevchenko National University of Kyiv
(64, Volodymyrs'ka Str., Kyiv 01601, Ukraine; e-mail: gorka@univ.kiev.ua)
[2] Bogolyubov Institute for Theoretical Physics, Nat. Acad. of Sci. of Ukraine
(14-b, Metrologichna Str., Kyiv 03680, Ukraine; e-mail: yusitenko@bitp.kiev.ua, pnd_ @ukr.net)

PACS 11.27.+d, 11.10.Kk

CASIMIR FORCE INDUCED ON A PLANE BY AN IMPENETRABLE FLUX TUBE OF FINITE RADIUS

A perfectly reflecting (Dirichlet) boundary condition at the edge of an impenetrable magnetic-flux-carrying tube of nonzero transverse size is imposed on the charged massive scalar matter field which is quantized outside the tube on a plane, which is transverse to the tube. We show that the vacuum polarization effects outside the tube give rise to a macroscopic force acting at the increase of the tube radius (if the magnetic flux is held steady).

K e y w o r d s: vacuum polarization, Casimir effect, magnetic vortex.

1. Introduction

Polarization of the vacuum of quantized matter fields under the influence of boundary conditions was studied intensively over more than six decades since Casimir [1] predicted a force between grounded metal plates: the prediction was that the induced vacuum energy in bounded spaces gave rise to a macroscopic force between bounding surfaces, see reviews in Refs. [2] and [3]. The Casimir force between grounded metal plates has now been measured quite accurately and agrees with the theoretical predictions (see, e.g., Refs. [4] and [5], as well as other publications cited in Refs. [2] and [3]).

In the present paper, we consider the vacuum energy which is induced by boundary conditions in space that is not bounded but, instead, is not simply connected, being an exterior to a straight infinitely long tube. This setup is inspired by the famous Aharonov–Bohm effect [6], and we are interested in the polarization of vacuum which is due to imposing a boundary condition at the edge of the tube carrying magnetic flux lines inside itself; this may be denoted as the Casimir–Aharonov–Bohm effect (see also [7]).

The vacuum polarization effects which are due to imposing the boundary conditions of various types at the cylindrical surfaces were extensively discussed in the literature, see [8]–[12]. In general, the Casimir effect in the presence of a single smooth object (cylinder or sphere) is rather different from that in the presence of two disjoint ones (e.g., plates): new divergences appear, and, to tame them, one has to sum the contributions of a quantized matter from both sides of the boundary surface, still this does not help in some cases to get rid completely of divergences, see [3] and references therein. In view of this, the conventional prescription which is to subtract the vacuum energy of the empty Minkowski space-time becomes insufficient for obtaining the meaningful results. The author of Ref. [13] proposes to define the Casimir energy for physical systems divided into classes: the difference in the vacuum energies of any two systems within the same class should be finite, then the finite Casimir energy has the universal interpretation as a vacuum energy with respect to the vacuum energy of a certain reference system which is common for the whole class. Following this proposition, we define a class of physical systems corresponding to the charged massive scalar field which is quantized outside an impenetrable tube with the magnetic flux of different values; the case of zero flux can be chosen as the reference system. As we shall show, the Casimir energy for this class is unambiguous and finite.

The temporal component of the energy-momentum tensor for a quantized charged scalar field $\Psi(x)$ in the flat space-time is given by the expression

$$T_{00}(x) = \frac{1}{2}\left[\partial_0\Psi^\dagger, \partial_0\Psi\right]_+ - \frac{1}{4}\left[\partial_0^2\Psi^\dagger, \Psi\right]_+ -$$

$$-\frac{1}{4}\left[\Psi^\dagger, \partial_0^2\Psi\right]_+ - \left(\xi - \frac{1}{4}\right)\boldsymbol{\nabla}^2\left[\Psi^\dagger, \Psi\right]_+, \qquad (1)$$

where $\boldsymbol{\nabla}$ is the covariant spatial derivative involving both affine and bundle connections, and the field operator in the case of a static background takes the form

$$\Psi(x^0,\mathbf{x}) = \sum\!\!\!\!\!\!\int_{\lambda} \frac{1}{\sqrt{2E_\lambda}} \times$$
$$\times \left[e^{-\mathrm{i}E_\lambda x^0}\psi_\lambda(\mathbf{x})\, a_\lambda + e^{\mathrm{i}E_\lambda x^0}\psi_{-\lambda}(\mathbf{x})\, b_\lambda^\dagger\right]; \qquad (2)$$

$a_\lambda^\dagger$ and a_λ ($b_\lambda^\dagger$ and b_λ) are the scalar particle (antiparticle) creation and destruction operators satisfying commutation relations; the wave functions $\psi_\lambda(\mathbf{x})$ form a complete set of solutions to the stationary Klein–Gordon equation

$$\left(-\boldsymbol{\nabla}^2 + m^2\right)\psi_\lambda(\mathbf{x}) = E_\lambda^2\psi(\mathbf{x}), \qquad (3)$$

m is the mass of the scalar particle; λ is the set of parameters (quantum numbers) specifying the state; $E_\lambda = E_{-\lambda} > 0$ is the energy of the state; symbol $\sum\!\!\!\!\!\!\int_\lambda$ denotes the summation over discrete and integration (with a certain measure) over continuous values of λ.

As is known for a long time [14–16], the energy-momentum tensor depends on the parameter ξ which couples Ψ to the scalar curvature of space-time even in the case of a vanishing curvature (see (1)); the conformal invariance is achieved in the limit of vanishing mass ($m = 0$) at $\xi = (d-1)(4d)^{-1}$, where d is the spatial dimension. Consequently, the density of the induced vacuum energy, which is given formally by expression

$$\varepsilon = \langle \mathrm{vac}|T_{00}(x)|\mathrm{vac}\rangle = \sum\!\!\!\!\!\!\int_{\lambda} E_\lambda\psi_\lambda^*(\mathbf{x})\,\psi_\lambda(\mathbf{x}) -$$
$$-(\xi - 1/4)\boldsymbol{\nabla}^2 \sum\!\!\!\!\!\!\int_{\lambda} E_\lambda^{-1}\psi_\lambda^*(\mathbf{x})\,\psi_\lambda(\mathbf{x}), \qquad (4)$$

depends on ξ as well. This poses a question: Can the physically measurable effects (e.g., the Casimir force) be dependent on ξ?

In the present paper, we consider a static background in the form of a cylindrically symmetric magnetic flux tube of finite transverse size. Hence, the covariant derivative is $\boldsymbol{\nabla} = \boldsymbol{\partial} - \mathrm{i}e\mathbf{V}$ with the vector potential possessing only one nonvanishing component given by

$$V_\varphi = \Phi/2\pi \qquad (5)$$

outside the tube. Here, Φ is the value of magnetic flux, and φ is the angle in the polar (r,φ) coordinates on a plane, which is transverse to the tube. The Dirichlet boundary condition at the edge of the tube ($r = r_0$) is imposed on the scalar field:

$$\psi_\lambda|_{r=r_0} = 0, \qquad (6)$$

i.e., the quantum matter is assumed to be perfectly reflected from the thence impenetrable flux tube.

As we shall see, the vacuum energy induced outside the flux tube on a plane, which is transverse to the tube, gives rise to a macroscopic force acting at the increase of the tube radius if the magnetic flux is held steady. Although the induced vacuum energy density is ξ-dependent, the Casimir force will be shown to be independent of ξ.

2. Vacuum Energy Density

The solution to (3) outside the magnetic flux tube can be obtained in terms of the cylindrical functions. The formal expression (4) for the vacuum energy density has to be renormalized by subtracting the contribution corresponding to the zero flux. Restricting ourselves to a plane orthogonal to the tube, we obtain (for details, see [17])

$$\varepsilon_{\mathrm{ren}} = \frac{1}{2\pi}\left\{\int_0^\infty dk\, k(k^2+m^2)^{1/2}[S(kr,kr_0) -\right.$$
$$-S(kr,kr_0)|_{\Phi=0}] - (\xi-1/4)\triangle\int_0^\infty dk\, k(k^2+m^2)^{-1/2}\times$$
$$\left.\times\,[S(kr,kr_0) - S(kr,kr_0)|_{\Phi=0}]\right\}, \qquad (7)$$

where

$$S(kr,kr_0) = \sum_{n\in\mathbb{Z}}\{[Y_{|n-e\Phi/2\pi|}(kr_0)J_{|n-e\Phi/2\pi|}(kr) -$$
$$-J_{|n-e\Phi/2\pi|}(kr_0)Y_{|n-e\Phi/2\pi|}(kr)]^2/$$
$$/(Y^2_{|n-e\Phi/2\pi|}(kr_0) + J^2_{|n-e\Phi/2\pi|}(kr_0))\}, \qquad (8)$$

$\mathbb{Z}$ is the set of integer numbers, $J_\mu(u)$ and $Y_\mu(u)$ are the Bessel functions of order μ of the first and second kinds, and $\triangle = \partial_r^2 + r^{-1}\partial_r$ is the radial part of the Laplacian operator on the plane.

Owing to the infinite range of the summation, the last expression is periodic in the flux Φ with a period

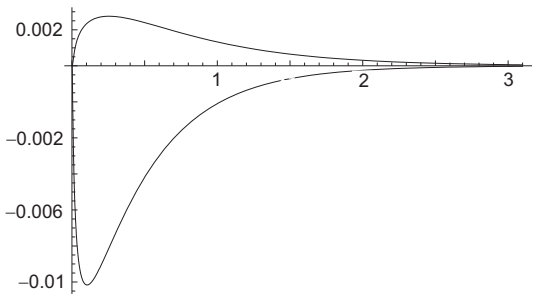

Fig. 1. Behavior of the $\alpha_+(x_0,x)$ (positive) and the $\alpha_-(x_0,x)$ (negative) functions for the case of $x_0=10^{-3}$. The variable x ($x>x_0$) is along the abscissa axis

equal to $2\pi e^{-1}$, i.e. the London flux quantum (we use units $c=\hbar=1$). Our further analysis concerns the case of $\Phi=(2n+1)\pi e^{-1}$, when each of the integrals in (7) is the most distinct from zero. Introducing the function [18]

$$G(kr,kr_0)=S(kr,kr_0)|_{\Phi=\pi e^{-1}}-S(kr,kr_0)|_{\Phi=0}, \quad (9)$$

we rewrite (7) in the dimensionless form

$$r^3\varepsilon_{\rm ren}=\alpha_+(mr_0,mr)-(\xi-1/4)r^3\triangle\frac{\alpha_-(mr_0,mr)}{r}, \quad (10)$$

where

$$\alpha_\pm(mr_0,mr)=\frac{1}{2\pi}\int\limits_0^\infty dz\,z\left[z^2+\left(\frac{mr_0}{\lambda}\right)^2\right]^{\pm1/2}G(z,\lambda z) \quad (11)$$

and $\lambda=r_0/r$ ($\lambda\in[0,1]$).

We follow the technique of numerical calculations developed in [17, 18] with some modifications. Notably, we perform the direct integration over consecutive periods of the $G(z,\lambda z)$ function using the Euler–Maclaurin integration formula [19]. This results in a sufficient decrease of the computation time.

Thereafter, we calculate the α_+ and α_- functions for the case of $mr_0=10^{-3}$ at a set of different distances from the axis of the tube. This allows us to obtain coefficients of the interpolation function, which is approximated in the form

$$\alpha_\pm(x_0,x)=\left[\pm e^{-2x}x^{1\mp1/2}\right]\times$$
$$\times\left[\left(\frac{x-x_0}{x}\right)^2\frac{P_3^\pm(x-x_0)}{x^3}\right]\frac{Q_3^\pm(x^2)}{R_3^\pm(x^2)}, \quad x>x_0, \quad (12)$$

where $x=mr$, $x_0=mr_0$, and $P_n^\pm(y)$, $Q_n^\pm(y)$, and $R_n^\pm(y)$ are polynomials in y of the n-th order with the x_0-dependent coefficients. The first factor in the square brackets in (12) describes the large-distance behavior in the case of the zero-radius tube (singular thread), second factor is the asymptotics at small distances from the tube edge, and the last factor is the intermediate part. Since the flux tube is impenetrable, the $\alpha_\pm$ functions vanish at $x\le x_0$. The behavior of the dimensionless $\alpha_\pm$ functions is presented in Fig. 1.

For the α_+ function, we estimate the relative error of the obtained result as 0.1%. It should be noted that nearly 95% of the integral value is obtained by the direct calculation, and only nearly 5% is the contribution from the interpolation. The integration in the case of the α_- function is performed more quickly and with a higher accuracy, as compared with the case of the α_+ function, because the former tends to zero more rapidly at large distances. In this case, the contribution from the interpolation can be estimated as 10^{-3}% of the total value.

We define the function [17]

$$\tilde\alpha_-(x_0,x)=r^3\triangle\frac{\alpha_-(x_0,x)}{r}=$$
$$=\alpha_-(x_0,x)-x\frac{\partial\alpha_-(x_0,x)}{\partial x}+x^2\frac{\partial^2\alpha_-(x_0,x)}{\partial x^2} \quad (13)$$

and present its behavior in Fig. 2.

We construct the dimensionless vacuum energy density at various values of the coupling to the spacetime curvature scalar (ξ),

$$r^3\varepsilon_{\rm ren}=\alpha_+(x_0,x)-(\xi-1/4)\tilde\alpha_-(x_0,x), \quad (14)$$

and present its behavior for $mr_0=10^{-3}$ in Fig. 3.

The behavior of the induced vacuum energy density, as the radius of the tube tends to zero, is of primary interest. To do a numerical calculation at $x_0<10^{-3}$ needs a significant computational time and is a rather complicated task. Nevertheless, we can make some general conclusions regarding the case of small x_0.

It seems plausible that this case with a decrease of the tube radius becomes more similar to the case of the tube of zero radius (singular thread) (see, e.g., Fig. 4). However, there are some peculiarities in the behavior in a vicinity of the tube. To discuss them,

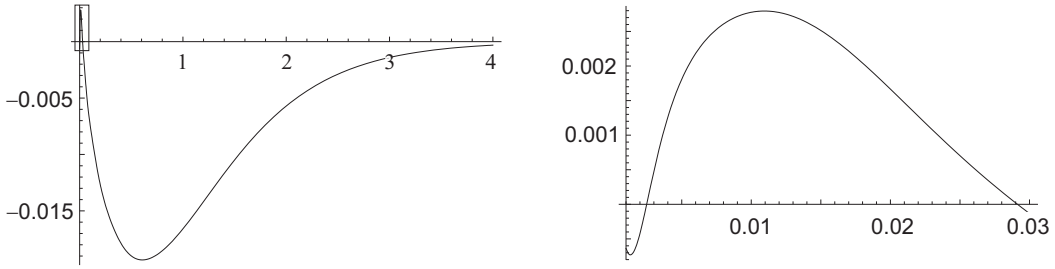

Fig. 2. Behavior of the $\tilde{\alpha}_-(x_0, x)$ function for $x_0 = 10^{-3}$. The region in a rectangle on the left figure is seen in the scaled-up form on the right figure. The variable x ($x > x_0$) is along the abscissa axis

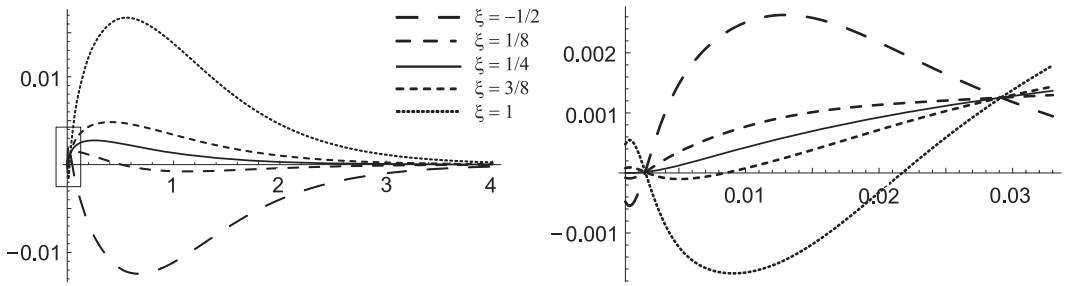

Fig. 3. Dimensionless vacuum energy density $r^3\varepsilon_{\rm ren}(x_0, x)$ at different values of coupling to the space-time curvature scalar for $x_0 = 10^{-3}$. The region in a rectangle on the left figure is seen in the scaled-up form on the right figure. The variable x ($x > x_0$) is along the abscissa axis

let us first recall the exact expressions corresponding to the case of the singular magnetic thread (see [20]):

$$\alpha_+(0,x)=\frac{x^3}{3\pi^2}\left\{\frac{\pi}{2}-2xK_0(2x)-K_1(2x)+\frac{K_2(2x)}{2x}-\right.$$
$$\left.-\pi x\left[K_0(2x)L_1(2x)+K_1(2x)L_0(2x)\right]\right\}, \quad (15)$$

$$\alpha_-(0,x)=\frac{x}{\pi^2}\left\{\frac{\pi}{2}-2xK_0(2x)-K_1(2x)-\right.$$
$$\left.-\pi x\left[K_0(2x)L_1(2x)+K_1(2x)L_0(2x)\right]\right\}, \quad (16)$$

$$\alpha_-(0,x)=-\frac{x}{\pi^2}\left[2xK_0(2x)+K_1(2x)\right], \quad (17)$$

where $K_\nu(u)$ and $L_\nu(u)$ are the Macdonald and the modified Struve functions of order ν. Consequently, in a vicinity of a thread, one gets

$$\alpha_+(0,x)=\frac{1-3x^2}{12\pi^2}, \quad x\ll 1 \quad (18)$$

$$\alpha_-(0,x)=-\frac{1-\pi x+(3-2\gamma-2\ln x)x^2}{2\pi^2}+O(x^3),$$
$$x\ll 1, \quad (19)$$

$$\tilde{\alpha}_-(0,x)=-\frac{1}{2\pi^2}+\frac{1+2\gamma+2\ln x}{2\pi^2}\,x^2+O(x^3),\ x\ll 1, \quad (20)$$

where γ is the Euler constant. Using the latter relations, we get the asymptotics of the renormalized vacuum energy density at small distances from the singular magnetic thread as

$$r^3\varepsilon_{\rm ren}^{\rm sing}=\frac{1}{12\pi^2}-\frac{x^2}{4\pi^2}-\left(\xi-\frac{1}{4}\right)\times$$
$$\times\left(-\frac{1}{2\pi^2}+\frac{1+2\gamma+2\ln x}{2\pi^2}x^2\right)+O(x^3),\ x\ll 1. \quad (21)$$

In contrast to (18) and (19), the $\alpha_\pm(x_0, x)$ functions in the case of nonzero radius vanish quadratically in a vicinity of the tube (see [17]):

$$\alpha_\pm(x_0,x)\big|_{x\to x_0}\sim O\left[(x-x_0)^2\right]. \quad (22)$$

To be more precise, we assume the asymptotics in the form, cf. (12),

$$\alpha_\pm(x_0,x)=\pm\frac{(x-x_0)^2}{x^2}f_\pm(x_0,x). \quad (23)$$

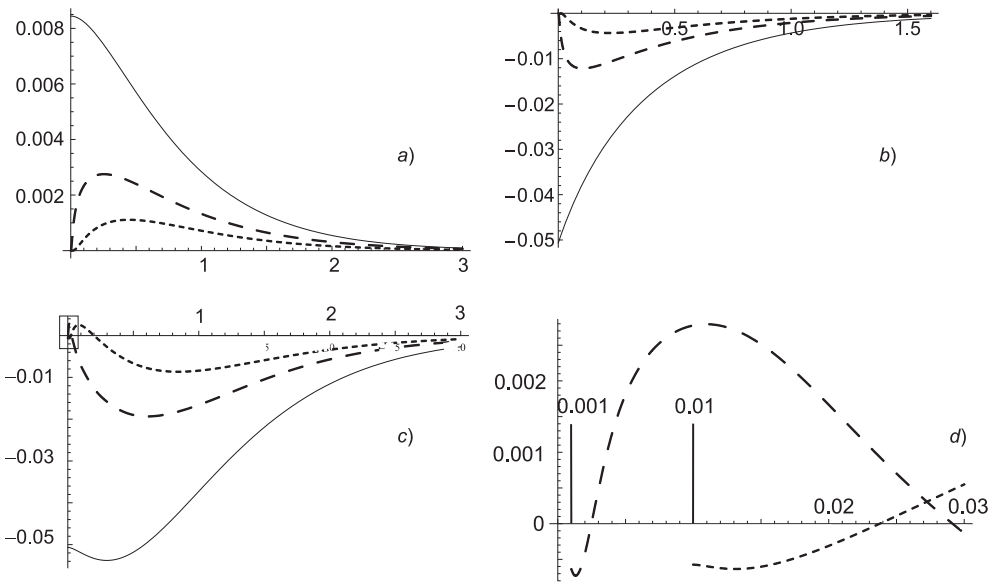

Fig. 4. Constituents of the dimensionless vacuum energy density: *a*) α_+, *b*) α_-, *c*) $\tilde{\alpha}_-$ for the case of $x_0 = 10^{-2}$ (dotted line), 10^{-3} (dashed line). The region in a rectangle on the *c*-figure is seen in the scaled-up form on the *d*-figure. The behavior of the corresponding functions for the case of a singular magnetic thread is presented by solid lines. The variable x ($x > 0$) is along the abscissa axis

Then we obtain

$$\tilde{\alpha}_-(x_0,x) = -(x-x_0)^2\frac{\partial^2}{\partial x^2}f_-(x_0,x) + \\ + \left(1 - 6\frac{x_0}{x} + 5\frac{x_0^2}{x^2}\right)x\frac{\partial}{\partial x}f_-(x_0,x) - \\ - \left(1 - 8\frac{x_0}{x} + 9\frac{x_0^2}{x^2}\right)f_-(x_0,x), \qquad (24)$$

with $\tilde{\alpha}_-(x_0,x_0) = -2f_-(x_0,x_0)$.

The $f_\pm(x_0,x)$ functions are adjusted as

$$f_+(0,x) = \frac{1-3x^2}{12\pi^2}, \quad x \ll 1, \qquad (25)$$

$$f_-(0,x) = \frac{1-\pi x + (3-2\gamma-2\ln x)x^2}{2\pi^2}, \ x \ll 1; \qquad (26)$$

consequently, we get

$$\tilde{\alpha}_-(x_0,x)\Big|_{\substack{x_0\to 0\\ x\to x_0}} = -\frac{1}{2\pi^2} + \frac{1+2\gamma+2\ln x}{2\pi^2}x^2 + \\ + \frac{4-\pi x}{\pi^2 x}x_0 + \frac{-9+4\pi x - 7x^2 + 2\gamma x^2 + 2x^2\ln x}{2\pi^2 x^2}x_0^2. \qquad (27)$$

The asymptotic behavior of the $\alpha_\pm$ and $\tilde{\alpha}_-$ functions with the use of (23)–(27) is presented in Fig. 5 in the case of a sufficiently small value of x_0. As one can see, this behavior is quite similar to that for the case of $x_0 = 10^{-3}$ (compare with Figs. 2 and 4). It should be noted that the $f_\pm(x_0,x)$ functions depend strongly on x_0.

3. Total Vacuum Energy and the Casimir Force

The total vacuum energy, which is induced on a plane outside the magnetic flux tube of finite radius, is

$$E \equiv \int_0^{2\pi} d\varphi \int_{r_0}^{\infty} \varepsilon_{\rm ren} r dr = 2\pi m \times \\ \times \left[\int_{x_0}^{\infty}\frac{\alpha_+(x_0,x)}{x^2}\,dx - \left(\xi - \frac{1}{4}\right)\int_{x_0}^{\infty}\frac{\tilde{\alpha}_-(x_0,x)}{x^2}\,dx\right]. \qquad (28)$$

In view of the relation

$$\int_{x_0}^{\infty}\frac{\tilde{\alpha}_-(x_0,x)}{x^2}\,dx = \left[\frac{\alpha_-(x_0,x)}{x} - \frac{\partial\alpha_-(x_0,x)}{\partial x}\right]\Big|_{x=x_0}, \qquad (29)$$

x_0	3/2	1	1/2	10^{-1}	10^{-2}	10^{-3}
$E/(2\pi m)$	5.013×10^{-12}	6.944×10^{-10}	2.068×10^{-7}	1.65×10^{-4}	0.0106	0.1486

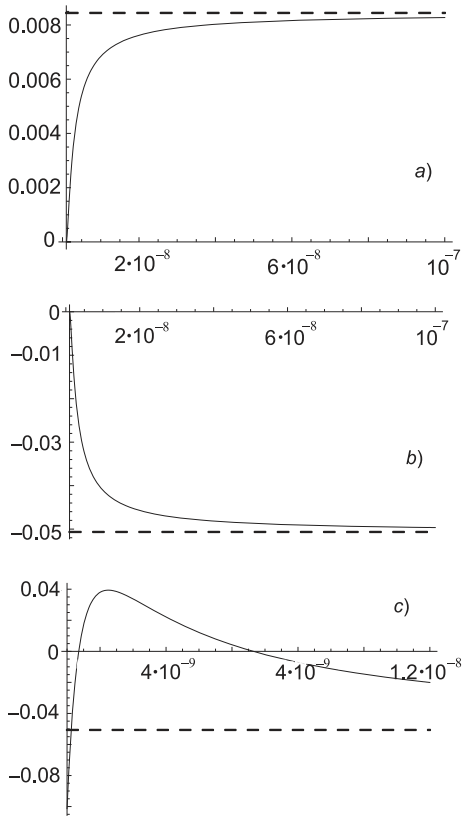

Fig. 5. Expected behavior of the constituents of the dimensionless vacuum energy density at small distances from the tube: *a*) α_+, *b*) α_-, *c*) $\tilde{\alpha}_-$ for the case of $x_0 = 10^{-9}$ (solid line). The behavior of the corresponding functions for the case of a singular magnetic thread is presented by the dashed lines. The variable x ($x > x_0$) is along the abscissa axis

which follows from (13) and relations (23) and (26), we conclude that the vacuum energy is independent of the coupling to the space-time curvature scalar (ξ):

$$E = 2\pi m \int\limits_{x_0}^{\infty} \frac{\alpha_+(x_0, x)}{x^2}\, dx. \tag{30}$$

This is in contrast to the case of a singular magnetic thread, when the total induced vacuum energy is divergent and ξ-dependent (see [20]):

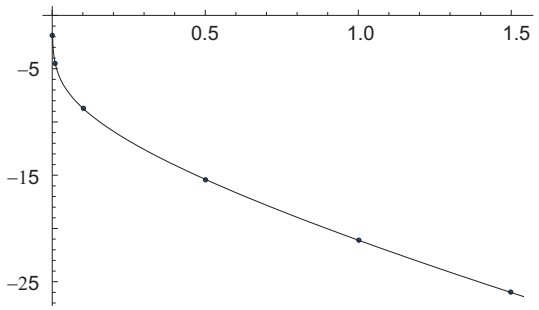

Fig. 6. Total vacuum energy as a function of the tube radius in the range $10^{-3} < x_0 < 3/2$. The variable x_0 is along the abscissa axis, the value of $\ln \frac{E}{2\pi m}$ is along the ordinate axis. Solid line interpolates the dots that have been calculated

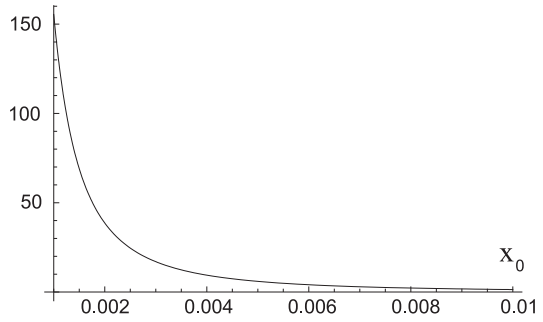

Fig. 7. Casimir force as a function of the tube radius. The variable x_0 is along the abscissa axis, the value of the dimensionless Casimir force $\frac{F(x_0)}{2\pi m^2}$ is along the ordinate axis

$$E^{\rm sing} \equiv \int\limits_0^{2\pi} d\varphi \int\limits_0^{\infty} \varepsilon_{\rm ren}^{\rm sing}\, r dr \sim 4m \left(\xi - \frac{1}{12}\right) \int\limits_0^{\infty} \frac{dx}{x^2}. \tag{31}$$

It is curious that the vacuum energy in this case is finite at $\xi = 1/12$, being equal to

$$E^{\rm sing}\big|_{\xi=1/12} = \frac{2m}{3\pi} \int\limits_0^{\infty} \left\{ \frac{\pi}{2} - \left(2x + \frac{1}{2x}\right) K_0(2x) - \right.$$

$$\left. - K_1(2x) - \pi x \left[K_0(2x) L_1(2x) + K_1(2x) L_0(2x)\right] \right\} \times$$

$$\times x\, dx = -0.01989 \times 2\pi m. \tag{32}$$

Although the vacuum energy E (30) is finite, its absolute value grows infinitely, as x_0 tends to zero (see (23) and (25)):

$$E|_{x_0\to 0} = m\left[\frac{1}{18\pi x_0} - \frac{x_0}{\pi}\ln x_0 + O(x_0^3)\right], \tag{33}$$

which is in accordance with the divergence of the vacuum energy in the case of a singular magnetic thread. To be more precise, relation (29) fails to yield zero in the case $x_0 = 0$. Therefore, the divergence of the vacuum energy in the latter case becomes ξ-dependent.

We present the values of vacuum energy E (30) for several values of the tube radius in the Table.

These results are also given in Fig. 6 on logarithmic scale, where the dots corresponding to the data in the table are joined with the help of the interpolation function,

$$\eta(x_0) = \ln\frac{E}{2\pi m}, \tag{34}$$

which can be taken in the form

$$\eta(x_0) = a_0 + \sum_i a_i x_0^{b_i} - \left(1 + \sum_j c_j x_0^{d_j}\right)\ln x_0. \tag{35}$$

Here, b_i and d_j are the positive adjustable constants.

To change the radius of a magnetic flux tube, one has to apply a work that is equal to the change of the total vacuum energy which is induced outside the tube. In the case of an infinitely small change of the radius, we have

$$\Delta E = 2\pi p\, r_0 \Delta r_0, \tag{36}$$

where p can be interpreted as the vacuum pressure, which acts from the exterior to the interior of the tube

$$p(x_0) = \frac{1}{2\pi r_0}\frac{dE}{dr_0} = m^3\frac{e^{\eta(x_0)}}{x_0}\frac{d\eta(x_0)}{dx_0}. \tag{37}$$

This results in the Casimir force acting from the interior to the exterior of the tube:

$$F(x_0) = -2\pi r_0 p(x_0) = -2\pi m^2 e^{\eta(x_0)}\frac{d\eta(x_0)}{dx_0}. \tag{38}$$

The behavior of the Casimir force is presented in Fig. 7.

As one can see, the Casimir force tends to increase the radius of the tube and to minimize the induced vacuum energy of the quantized scalar field. Certainly, our conclusion is obtained under the assumption that the magnetic flux inside the impenetrable tube remains invariable with a variation of the tube radius.

4. Summary

In the present paper, we consider the vacuum polarization effects that are induced in a scalar matter by imposing a perfectly reflecting (Dirichlet) boundary condition at the edge of an impenetrable finite-radius tube, which carries magnetic flux lines inside itself. Restricting ourselves to a plane, which is orthogonal to the tube, we define the induced vacuum energy density (see (7) and (8)) and analyze numerically its behavior as a function of the distance from the tube for the magnetic flux equal to half of the London flux quantum ($\Phi = \pi e^{-1}$), the tube radius equal to $r_0 = 10^{-3}m^{-1}$, and different values of the coupling to the space-time curvature scalar (ξ) (see Fig. 3). The emergence of the energy density, as well as of other components of the energy-momentum tensor, in the vacuum can lead to various semiclassical gravitational effects, which were estimated under the neglect of the tube radius in [21].

The present paper summarizes and extends our previous study in [17, 18], and this allows us to draw conclusions about the behavior of the total induced vacuum energy, i.e. the density integrated over the whole plane, and the Casimir force as functions of the tube radius. We find that the total induced vacuum energy is finite and independent of ξ, as long as the tube radius is taken into account. Although the values of total induced vacuum energy are negligible for $r_0 \sim m^{-1}$ (see also [18]) being of order $10^{-10}\times 2\pi m$, they are of order $10^{-1}\times 2\pi m$ for $r_0 \sim 10^{-3}m^{-1}$, see the Table and Fig. 6. The induced vacuum energy gives rise to the Casimir force which is directed from the exterior to the interior of the tube. The force acts at an increase of the tube radius and a decrease of the induced vacuum energy, if the magnetic flux is held constant[1]. The force takes considerable values at small values of the tube radius and actually disappears otherwise: it is, e.g., $10^2\times 2\pi m^2$ at $r_0 \sim 10^{-3}m^{-1}$ and $10^{-3}\times 2\pi m^2$ at $r_0 \sim 10^{-1}m^{-1}$. The behavior of the force as a function of the tube radius is illustrated by Fig. 7.

[1] As to the energy stored inside the tube, it is the purely classical energy of the magnetic field. Its behavior at an increase of the tube radius as the magnetic flux is held constant can be different depending on the details of the magnetic field configuration. Mild assumptions as to the smoothness of the configuration yield that the energy is either constant or decreasing at most as $\sim r_0^{-2}$.

It should be noted that the Casimir force in our case is caused by the boundary conditions imposed at the boundary enclosing a magnetic flux. The force is periodic in the flux value with a period equal to the London flux quantum, attaining its maximal value at $\Phi = (2n+1)\pi e^{-1}$ and vanishing at $\Phi = 2n\pi e^{-1}$ ($n \in \mathbb{Z}$).

The work was partially supported by special program "Microscopic and phenomenological models of fundamental physical processes in micro- and macroworld" of the Department of Physics and Astronomy of the National Academy of Sciences of Ukraine.

1. H.B.G. Casimir, Proc. Kon. Ned. Akad. Wetenschap. B **51**, 793 (1948); Physica **19**, 846 (1953).
2. K.A. Milton, *The Casimir Effect: Physical Manifestations of Zero-Point Energy* (World Scientific, River Edge, 2001).
3. M. Bordag, G.L. Klimchitskaya, U. Mohideen, and V.M. Mostepanenko, *Advances in the Casimir Effect* (Oxford Univ. Press, Oxford, 2009).
4. S.K. Lamoreax, Phys. Rev. Lett. **78**, 5 (1997).
5. G. Bressi, G. Carugno, R. Onofrio, and G. Ruoso, Phys. Rev. Lett. **88**, 041804 (2002).
6. Y. Aharonov and D. Bohm, Phys. Rev. **115**, 485 (1959).
7. Yu. A. Sitenko and A.Yu. Babansky, Mod. Phys. Lett. A **13**, 379 (1998).
8. L.L. DeRaad, Jr. and K.A. Milton, Ann. Phys. (N.Y.) **136**, 229 (1981).
9. P. Gosdzinsky and A. Romeo, Phys. Lett. B **441**, 265 (1998).
10. N. Graham, R.L. Jaffe, V. Khemani, M. Quandt, M. Scandurra, and H. Weigel, Phys. Lett. B **572**, 196 (2003).
11. G. Barton, Phys. Rev. D **73**, 065018 (2006).
12. I. Cavero-Pelaez, K.A. Milton, and K. Kirsten, J. Phys. A: Math. Theor. **40**, 3607 (2007).
13. M. Schaden, Phys. Rev. A **73**, 042102 (2006).
14. R. Penrose, in: *Relativity, Groups and Topology*, edited by B.S. DeWitt, C. DeWitt (Gordon and Breach, New York, 1964).
15. N.A. Chernikov and E.A. Tagirov, Ann. Inst. Henri Poincaré A **9**, 109 (1968).
16. C.G. Callan, S. Coleman, and R. Jackiw, Ann. Phys. (N.Y.) **59**, 42 (1970).
17. V.M. Gorkavenko, Yu.A. Sitenko, and O.B. Stepanov, Int. J. Mod. Phys. A: **26**, 3889 (2011).
18. V.M. Gorkavenko, Yu.A. Sitenko, and O.B. Stepanov, J. Phys. A: Math. Theor. **43**, 175401 (2010).
19. E.T. Whittaker and G.N. Watson, *The Euler-Maclaurin Expansion* (Cambridge Univ. Press, Cambridge, 1990).
20. Yu.A. Sitenko and V.M. Gorkavenko, Phys. Rev. D **67**, 085015 (2003).
21. V.M. Gorkavenko and A.V. Viznyuk, Phys. Lett. B **604**, 103 (2004).

Received 27.09.12

В.М. Горкавенко, Ю.О. Ситенко, О.Б. Степанов

СИЛА КАЗИМІРА, ЩО ІНДУКУЄТЬСЯ НА ПЛОЩИНІ НЕПРОНИКЛИВОЮ МАГНІТНОЮ ТРУБКОЮ СКІНЧЕННОГО РАДІУСА

Р е з ю м е

Розглядається задача поляризації вакууму масивного заряджeного скалярного поля матерії на площині, перпендикулярно до якої проходить непрониклива для поля матерії трубка скінченного радіуса з магнітним потоком всередині. На поверхні трубки на поле матерії накладається гранична умова типу Діріхле. Показано, що ефекти поляризації вакууму поля матерії приводять до появи макроскопічної сили, що намагається збільшити радіус трубки. Розрахунок проведений в припущенні збереження магнітного потоку всередині трубки.